PRAMANA
— journal of
physics

Vol. 73, No. 6
December 2009
pp. 1059–1072

Stability of $^{244-260}$Fm isotopes against alpha and cluster radioactivity

K P SANTHOSH[1,*], R K BIJU and SABINA SAHADEVAN
P.G. Department of Physics & Research Centre, Payyanur College,
Payyanur 670 327, India
[1]Present address: School of Pure and Applied Physics, Kannur University,
Payyanur Campus, Payyanur 670 327, India
*Corresponding author. E-mail: kpsanthosh@eth.net

MS received 30 December 2008; revised 30 May 2009; accepted 22 June 2009

Abstract. Taking Coulomb and proximity potentials as the interacting barrier we have studied the cold valley in the radioactive decay of $^{244-260}$Fm isotopes. It is found that in addition to alpha particle minima, other minima occur at S, Ar and Ca clusters. We have computed the half-lives and other characteristics of different clusters emitted from these parents treating parent, daughter and emitted cluster as spheres. Our study reveals that most of these parents are unstable against alpha and heavy cluster (^{46}Ar, ^{48,50}Ca) emissions and stable against light cluster emission, except ^{8}Be from $^{244-248}$Fm isotopes. The most probable clusters from these parents are predicted to be ^{46}Ar, ^{48,50}Ca which indicate the role of doubly or near doubly magic clusters ($Z = 20, N = 28$) and also stress the role of doubly magic ^{208}Pb daughter. The computed half-lives for alpha decay are in good agreement with the experimental data. It is found that the presence of neutron excess in the parent nuclei slows down the cluster decay process. The effect of quadrupole (β_2) and hexadecapole (β_4) deformations of parent and fragments on half-lives are also studied. It is found that inclusion of β_2 and β_4 reduces the height and shape of the barrier (increases barrier penetrability) and hence the half-life decreases.

Keywords. Cluster decay; alpha decay.

PACS Nos 23.60.+e; 23.70.+j; 27.90.+b

1. Introduction

Cluster radioactivity is a rare, cold (neutron-less) process, intermediate between alpha decay and spontaneous fission. It is the spontaneous decay of radioactive nuclei with the emission of fragments heavier than alpha particle. This phenomenon was first predicted by Sandulescu *et al* [1] in 1980 on the basis of quantum mechanical fragmentation theory [2]. Later this was confirmed by Rose and Jones [3] in 1984. After the observation of cluster radioactivity, lots of efforts have been done on both experimental and theoretical fronts for understanding the physics of

cluster radioactivity. At present about 20 parent nuclei from ^{221}Fr to ^{242}Cm emitting clusters ranging from ^{14}C to ^{34}Si are confirmed [4]. For e.g. ^{14}C from ^{221}Fr, $^{221-226}$Ra and ^{226}Th, ^{20}O from ^{228}Th, ^{24,26}Ne from ^{230,232}Th and ^{232,234}U, ^{28,30}Mg from ^{238}Pu, ^{32,34}Si from ^{238}Pu and ^{241}Am etc. are observed. Many theoretical models have been introduced for explaining cluster radioactivity; these models can be broadly classified as fission and cluster models. In fission model [1,5–16] the nucleus deforms continuously as it penetrates the nuclear barrier and reaches the scission configuration after running down the Coulomb barrier. In cluster model [17–21], the cluster is assumed to be preformed in the parent nuclei before it penetrates the nuclear interacting barrier. In the cluster decay studies cluster-like shapes are preferred for very high asymmetric mass splitting and fissioning shapes are most suitable for less asymmetric and symmetric mass splitting.

In the present paper, based on the concept of cold valley in cold fission and fusion, we have investigated the cluster decay process in $^{244-260}$Fm isotopes. Fermium is one of the transuranium elements, which lies beyond uranium in the periodic table. It is the eighth discovered transuranium element of the actinide series and was identified by Ghiorso and co-workers in 1952 in the debris of a thermonuclear explosion in the Pacific during a work involving the University of California Radiation Laboratory, Argonne National Laboratory and Los Alamos National Laboratory. Sixteen isotopes of fermium are known to exist. All isotopes of fermium are radioactive. Fermium does not occur naturally in the Earth's crust. The isotopes of fermium are prepared by neutron irradiation of Pu, and a sequence of neutron capture reactions and beta decay process occurs leading from Pu through Am, Cm, Bk, Cf and Es to Fm [22]. The most stable isotope is ^{257}Fm, with a half-life of about 100.5 days and it was produced by prolonged bombardment of Cm with neutron in a reactor [23]. The isotope ^{250}Fm, with a half-life of 30 min, has been shown to be a decay product of element ^{254}102. The isotope ^{255}Fm was produced at ORNL in Oak Ridge, USA. The cross-sections of fermium isotopes show an interesting pattern, i.e. the values for isotopes of mass 255 and less are at least one order of magnitude higher than that of ^{256}Fm and ^{257}Fm [24].

In previous works, Santhosh *et al* [25–28] proposed the Coulomb and proximity potential models to study cluster radioactivity in various proton-rich parents with $Z = 56$–64 and $N = 56$–72, leading to doubly magic ^{100}Sn. The predicted logarithmic half-life [14] for ^{12}C emission from ^{112}Ba isotope was 3.78 s which is in good agreement with the value 3.75 s reported by Guglielmetti *et al* [29]. However, this result could not be reproduced in the experiments [30] carried out at GSI in 1997. Hence, the above half-life values are taken as the experimental lower limit. This decay which was earlier considered as ground-state decay now seems to be the decay from the corresponding excited compound system [31]. This model is modified [32] by incorporating the ground-state deformations β_2 and β_4 of the parent and daughter treating cluster as a sphere and the effect of deformation on the half-lives are studied. We also studied the cold valleys in the radioactive decay of $^{248-254}$Cf isotopes [33] and the computed alpha decay half-life values which closely agree with the experimental data. Recently, we have proposed a semi-empirical model [34] for describing alpha and cluster radioactivity and the formula is applied to parents exhibiting cluster decay and alpha decay. In this work we would like to explore the stability of $^{244-260}$Fm isotopes against alpha and heavy cluster emissions taking

interacting barrier as the sum of Coulomb and proximity potentials. The effect of quadrupole and hexadecapole deformations of parents and fragments on half-life is also studied. We would like to point out that the multipole deformation and orientation of nuclei in cluster radioactivity was being done by Gupta and co-workers [35–37] since 2007. The details of the model are given in §2. Section 3 describes the results, discussion and conclusion.

2. The model

The interacting potential barrier for a parent nucleus exhibiting exotic decay is given by

$$V = \frac{Z_1 Z_2 e^2}{r} + V_{\rm p}(z) + \frac{\hbar^2 \ell(\ell+1)}{2\mu r^2}, \quad \text{for } z > 0. \tag{1}$$

Here Z_1 and Z_2 are the atomic numbers of the daughter and the emitted clusters, r is the distance between fragment centres, z is the distance between the near surfaces of the fragments, ℓ is the angular momentum, μ is the reduced mass and $V_{\rm p}$ is the proximity potential given by Blocki *et al* [38],

$$V_{\rm p}(z) = 4\pi\gamma b \left[\frac{C_1 C_2}{(C_1 + C_2)}\right] \Phi\left(\frac{z}{b}\right). \tag{2}$$

Equations (1) and (2) are for spherical nuclei. The nuclear surface tension coefficient,

$$\gamma = 0.9517[1 - 1.7826(N-Z)^2/A^2] \quad \text{MeV/fm}^2, \tag{3}$$

where N, Z and A represent neutron, proton and mass number of the parent, Φ represents the universal proximity potential given as [39]

$$\Phi(\varepsilon) = -4.41\mathrm{e}^{-\varepsilon/0.7176}, \quad \text{for } \varepsilon \geq 1.9475 \tag{4}$$

$$\Phi(\varepsilon) = -1.7817 + 0.9270\varepsilon + 0.0169\varepsilon^2 - 0.05148\varepsilon^3, \quad \text{for } 0 \leq \varepsilon \leq 1.9475, \tag{5}$$

with $\varepsilon = z/b$, where the width (diffuseness) of the nuclear surface $b \approx 1$ and Siissmann central radii C_i of fragments related to sharp radii R_i as

$$C_i = R_i - \left(\frac{b^2}{R_i}\right). \tag{6}$$

For R_i we use a semi-empirical formula in terms of mass number A_i as [38]

$$R_i = 1.28A_i^{1/3} - 0.76 + 0.8A_i^{-1/3}. \tag{7}$$

Using one-dimensional WKB approximation, the barrier penetrability P is given as

$$P = \exp\left\{-\frac{2}{\hbar}\int_a^b \sqrt{2\mu(V-Q)}\mathrm{d}z\right\}. \tag{8}$$

Here the mass parameter is replaced by the reduced mass $\mu = mA_1A_2/A$, where m is the nucleon mass and A_1, A_2 are the mass numbers of the daughter and emitted clusters respectively. The turning points a and b are determined from the equation $V(a) = V(b) = Q$. The above integral can be evaluated numerically or analytically, and the half-life is given by

$$T_{1/2} = \left(\frac{\ln 2}{\lambda}\right) = \left(\frac{\ln 2}{\upsilon P}\right), \tag{9}$$

where $\upsilon = (\omega/2\pi) = (2E_\mathrm{v}/h)$ represents the number of assaults on the barrier per second and λ is the decay constant. E_v the empirical zero point vibration energy is given as [6]

$$E_\mathrm{v} = Q\left\{0.056 + 0.039\exp\left[\frac{(4-A_2)}{2.5}\right]\right\}, \quad \text{for } A_2 \geq 4. \tag{10}$$

The Coulomb interaction between the two deformed and oriented nuclei taken from [40] with higher multipole deformation included [41,42] is given as

$$V_\mathrm{C} = \frac{Z_1Z_2e^2}{r} + 3Z_1Z_2e^2\sum_{\lambda,i=1,2}\frac{1}{2\lambda+1}\frac{R_{0i}^\lambda}{r^{\lambda+1}}Y_\lambda^{(0)}(\alpha_i) \times\left[\beta_{\lambda i} + \frac{4}{7}\beta_{\lambda i}^2Y_\lambda^{(0)}(\alpha_i)\delta_{\lambda,2}\right] \tag{11}$$

with

$$R_i(\alpha_i) = R_{0i}\left[1 + \sum_\lambda \beta_{\lambda i}Y_\lambda^0(\alpha_i)\right], \tag{12}$$

where $R_{0i} = 1.28A_i^{1/3} - 0.76 + 0.8A_i^{-1/3}$. Here α_i is the angle between the radius vector and symmetry axis of the ith nuclei (see figure 1 of ref [41]). Note that the quadrupole interaction term proportional to $\beta_{21}\beta_{22}$ is neglected because of its short-range character.

3. Results, discussion and conclusion

We have done our calculations taking potential barrier as the sum of Coulomb potential, proximity potential and centrifugal potential for the touching configuration and for the separated fragments. For the pre-scission (overlap) region, simple power-law interpolation [43] is used. The inclusion of proximity potential reduces the height of the barrier which closely agrees with the experimental values. The possibility to have a cluster emission process is

$$Q = M(A, Z) - M(A_1, Z_1) - M(A_2, Z_2) > 0, \tag{13}$$

where $M(A, Z), M(A_1, Z_1)$ and $M(A_2, Z_2)$ are the atomic masses of the parent, daughter and cluster respectively. The barrier penetrability is very sensitive to Q value and the Q values are computed using experimental binding energies of Audi *et al* [44] and some masses are taken from the table of KUTY [45].

The proximity potential was first used by Shi and Swiatecki [43] in an empirical manner and has been quiet extensively used over a decade by Gupta and coworkers [20] in the preformed cluster model (PCM) which is based on the pocket formula of Blocki *et al* [38] given as

$$\Phi(\varepsilon) = -\left(\frac{1}{2}\right)(\varepsilon - 2.54)^2 - 0.0852(\varepsilon - 2.54)^3, \quad \text{for } \varepsilon \leq 1.2511 \tag{14}$$

$$\Phi(\varepsilon) = -3.437 \exp\left(\frac{-\varepsilon}{0.75}\right), \quad \text{for } \varepsilon \geq 1.2511. \tag{15}$$

In the present model, another formulation of proximity potential [39] given by eqs (4) and (5) has been used. In this model, cluster formation probability is taken as unity for all clusters irrespective of their masses and so the present model differs from preformed cluster model by a factor P_0, the cluster formation probability. The assault frequency, ν, is calculated for each parent–cluster combination which is associated with zero point vibration energy but Shi and Swiatecki [43] get ν empirically, unrealistic values 10^{22} for even A parent and 10^{20} for odd A parent.

The concept of cold valley was introduced in relation to the structure of minima in the so-called driving potential, which is defined as the difference between the interaction potential and the decay energy (Q value) of the reaction. The driving potential is given by

$$V = \frac{Z_1 Z_2 e^2}{r} + V_{\mathrm{p}}(z) + \frac{\hbar^2 \ell(\ell+1)}{2\mu r^2} - Q. \tag{16}$$

The driving potential of a compound nucleus is calculated for all possible cluster–daughter combinations as a function of mass and charge asymmetries. For every fixed mass pair, a pair of charges is singled out among all possible configurations for which driving potential is minimum. In the present paper the calculations are done for the touching configuration of the fragments.

Figures 1 represents the plots of driving potential vs. A_2, the mass of one fragment for ^{244}Fm isotopes with and without the inclusion of proximity potential. From these plots it is clear that the inclusion of proximity potential does not change the position of minima but minima become deeper. The minima in driving potential represent the most probable decay which is due to the shell closure of one or both fragments. In these figures it is obvious that ^{4}He, ^{8,10}Be, ^{12,14,16}C, ^{18,20,22}O, ^{28,30}Mg, ^{42,44,46}Ar, ^{48,50}Ca etc. have minimum driving potential.

In figure 1, as we move towards the heavy cluster region we can see a deep region consisting of several comparable minima, which is centred on ^{208}Pb (for e.g. ^{38}Ar + ^{206}Pb, ^{40}Ar + ^{204}Pb) showing the role of double magicity of the daughter nuclei with $N = 126$ and $Z = 82$. As we move towards the symmetric fission region, we

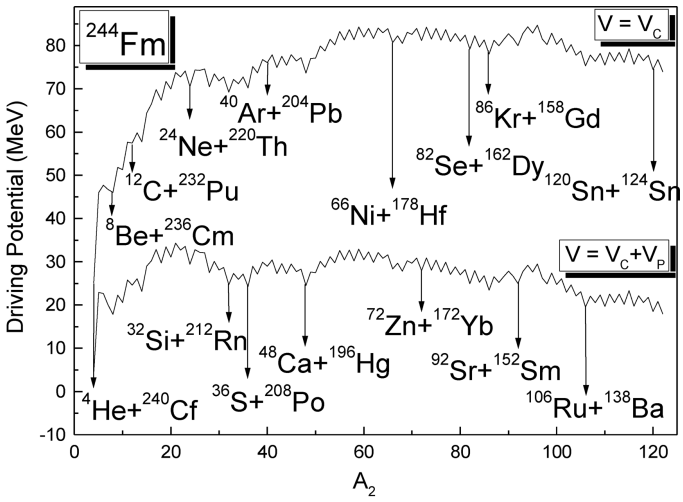

Figure 1. The plot of driving potential vs. A_2, the mass of one fragment for ^{244}Fm with and without proximity potential.

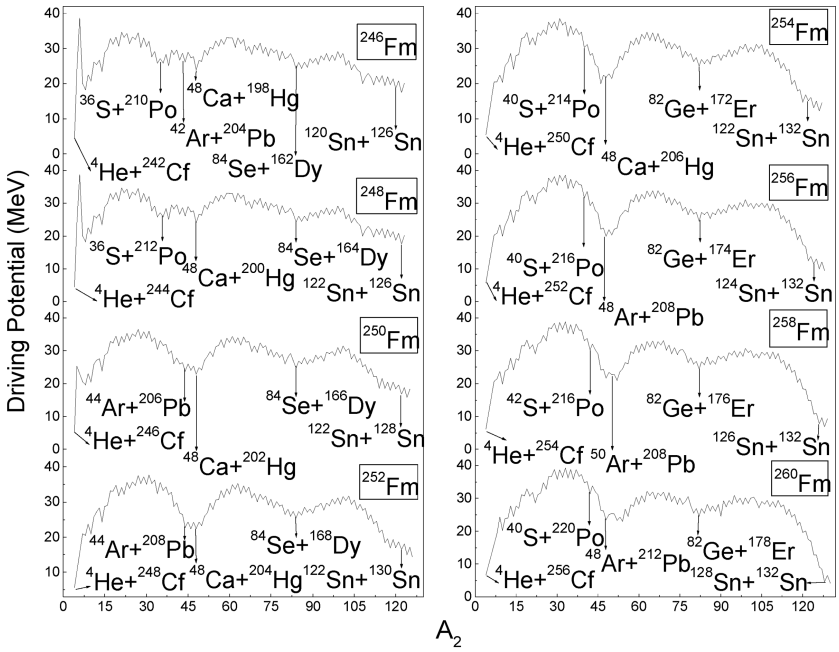

Figure 2. The plot of driving potential vs. A_2, the mass of one fragment for $^{246-260}$Fm by including proximity potential.

can see that the driving potential decreases with increase in mass number (A_2), i.e. in this region there is a chance for symmetric fission to occur (for e.g. ^{120}Sn + ^{124}Sn). This also stresses the role of double or near double magicity of the fragments ^{132}Sn.

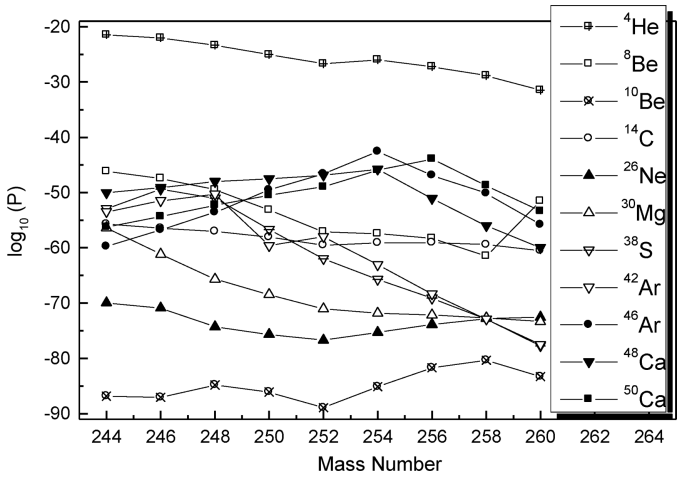

Figure 3. Variation of logarithm of barrier penetrability with mass number of the parent for various clusters emitting from $^{244-260}$Fm isotopes.

Figure 2 represents the plot of driving potential vs. A_2, the mass of one fragment for $^{246-260}$Fm isotopes with the inclusion of proximity potential. In this figure we can see a deep valley consisting of several comparable minima and is centred on ^{208}Pb the same as that of figure 1 (for e.g. ^{42}Ar + ^{208}Pb in ^{246}Fm, ^{42}Ar + ^{206}Pb in ^{248}Fm, ^{44}Ar + ^{206}Pb in ^{250}Fm, ^{44}Ar + ^{208}Pb in ^{252}Fm, ^{46}Ar + ^{208}Pb in ^{254}Fm, ^{48}Ar + ^{208}Pb in ^{256}Fm, ^{50}Ar + ^{208}Pb in ^{258}Fm, ^{48}Ar + ^{212}Pb in ^{260}Fm etc.) which stresses the role of double magicity of the daughter nuclei with $N = 126$ and $Z = 82$. In the symmetric fission region, we can see that the driving potential decreases with increase in mass number (A_2). The minima in driving potential is obtained around ^{132}Sn (for e.g. ^{120}Sn + ^{126}Sn in ^{246}Fm, ^{122}Sn + ^{126}Sn in ^{248}Fm, ^{122}Sn + ^{128}Sn in ^{250}Fm, ^{122}Sn + ^{130}Sn in ^{252}Fm, ^{122}Sn + ^{132}Sn in ^{254}Fm, ^{124}Sn + ^{132}Sn in ^{256}Fm, ^{126}Sn + ^{132}Sn in ^{258}Fm, ^{128}Sn + ^{132}Sn in ^{260}Fm) which again stresses the role of double magicity of the fragments ^{132}Sn with $N = 82$ and $Z = 50$.

Tables 1 and 2 give the computed half-life values (Present I), barrier penetrability and other characteristics of $^{244-260}$Fm isotopes with half-life $T_{1/2} \leq 10^{30}$ s. We would like to point out that with the present available experimental techniques, the half-life values up to 10^{30} s are possible for measurement. For computing half-life values the interacting potential is taken as the sum of Coulomb and proximity potentials, i.e. $V_{\rm C} + V_{\rm p}$. The angular momentum ℓ carried away in the cluster decay process, appearing in eq. (1) is very small ($\approx 5h$) and its contribution to half-life is also shown to be small [6,27] which is decided by the spin-parity conservation. Therefore, in the present work the calculations are done assuming zero angular momentum transfers. The computed alpha decay half-lives (Present I) are compared with experimental data taken from Royer [46] and the standard deviation is found to be 1.26. We have improved our alpha decay half-life predictions by including zero point vibration energy, $E_{\rm v}$, in barrier penetrability calculations (eq. (8)) with new turning points determined by $V(a) = V(b) = Q + E_{\rm v}$. The predicted half-lives (Present II) are in good agreement with experimental data (e.g. in ^{250}Fm

Table 1. The computed half-life values, barrier penetrability and other characteristics of $^{244-250}$Fm isotopes with zero angular momentum transfers. Here the interacting potential is taken as $V_C + V_P$.

Parent nuclei	Emitted cluster	Daughter nuclei	Q-value (MeV)	Penetrability P	Decay constant	$\log_{10}(T_{1/2})$	
						Present I	Present II
^{244}Fm	^{4}He	^{240}Cf	8.555	3.42E-22	0.134	0.713	0.315
	^{8}Be	^{236}Cm	16.178	7.11E-47	3.56E-26	25.290	24.773
	^{12}C	^{232}Pu	30.644	2.72E-50	2.32E-29	28.476	27.876
	^{32}Si	^{212}Rn	101.751	1.51E-47	4.16E-26	25.221	24.007
	^{34}Si	^{210}Rn	98.837	1.15E-51	3.08E-30	29.352	28.162
	^{36}S	^{208}Po	118.543	4.24E-47	1.36E-25	24.707	22.441
	^{38}S	^{206}Po	114.053	1.16E-53	3.57E-32	31.288	29.969
	^{42}Ar	^{202}Pb	129.364	3.08E-54	1.08E-32	31.808	29.441
	^{48}Ca	^{196}Hg	145.052	8.38E-51	3.30E-29	28.323	26.756
^{246}Fm	^{4}He	^{242}Cf	8.375	9.02E-23	3.50E-02	1.300	0.913
	^{8}Be	^{238}Cm	15.798	3.53E-48	1.72E-27	26.604	26.090
	^{12}C	^{234}Pu	29.790	2.40E-52	2.00E-31	30.541	29.949
	^{32}Si	^{214}Rn	98.540	1.13E-52	3.01E-31	30.363	29.226
	^{34}Si	^{212}Rn	98.757	1.73E-51	4.63E-30	29.175	27.980
	^{36}S	^{210}Po	116.757	9.67E-50	3.06E-28	27.356	25.947
	^{38}S	^{208}Po	115.871	3.99E-50	1.25E-28	27.743	26.325
	^{48}Ca	^{198}Hg	145.309	7.91E-50	3.11E-28	27.348	25.776
^{248}Fm	^{4}He	^{244}Cf	8.001	4.50E-24	1.65E-03	2.622	2.262
	^{8}Be	^{240}Cm	15.239	3.19E-50	1.50E-29	28.665	28.170
	^{38}S	^{210}Po	114.720	9.35E-52	2.91E-30	29.378	28.009
	^{40}S	^{208}Po	113.626	1.80E-52	3.36E-31	30.281	28.902
	^{46}Ar	^{202}Pb	127.560	2.56E-54	8.83E-33	31.895	29.309
	^{48}Ca	^{200}Hg	145.625	9.13E-49	3.60E-27	26.284	24.666
	^{50}Ca	^{198}Hg	142.431	5.23E-53	2.02E-31	30.536	29.031
^{250}Fm	^{4}He	^{246}Cf	7.557	9.28E-26	3.22E-05	4.333	3.996
	^{40}S	^{210}Po	112.877	1.21E-53	3.69E-32	31.274	29.913
	^{42}Cl	^{208}Bi	120.733	1.40E-53	4.59E-32	31.179	29.696
	^{44}Ar	^{206}Pb	130.537	1.17E-48	4.12E-27	26.225	24.819
	^{46}Ar	^{204}Pb	128.904	2.74E-50	9.57E-29	27.860	26.436
	^{48}Ca	^{202}Hg	145.635	3.00E-48	1.19E-26	25.767	24.119
	^{50}Ca	^{200}Hg	143.149	3.05E-51	1.18E-29	28.769	27.221

experimental $\log_{10}(T_{1/2}) = 3.25$ and present value = 3.99; in ^{254}Fm experimental $\log_{10}(T_{1/2}) = 4.19$ and present value = 4.99) and the estimated standard deviation is found to be 0.89. We have extended this calculation to all clusters up to ^{70}Ni and these are presented in tables 1 and 2 as Present II. Our study reveals that these parents are unstable against alpha and heavy cluster (for ^{46}Ar, ^{48,50}Ca) emissions and stable against light cluster emission, excluding ^{8}Be from $^{244-248}$Fm isotopes. In alpha and cluster radioactivity it is found that the half-life has the minimum value for those decays which lead to doubly magic daughters [47]. We have

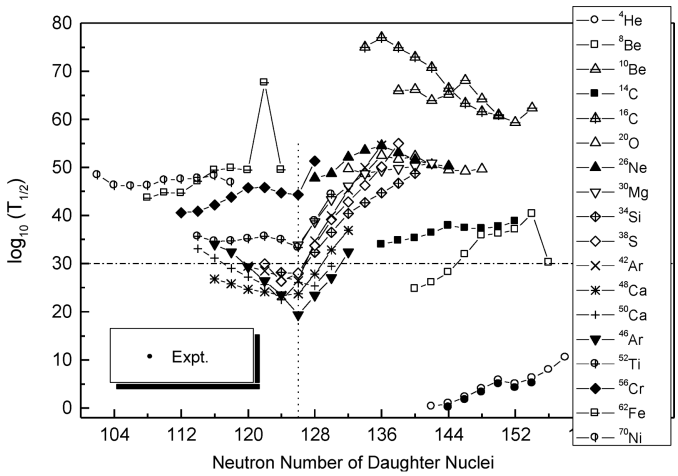

Figure 4. Computed half-life vs. neutron number of daughter nuclei for $^{244-260}$Fm isotopes emitting clusters ranging from ^{4}He to ^{70}Ni. The computed alpha decay half-life is compared with experimental data [46]. Horizontal dotted line represents the experimental limit. Half-life is in seconds.

identified that ^{44}Ar ($\log_{10} T_{1/2} = 24.065$ s) from ^{252}Fm, ^{46}Ar ($\log_{10} T_{1/2} = 20.306$ s) from ^{254}Fm and ^{48}Ar ($\log_{10} T_{1/2} = 21.724$ s) from ^{256}Fm, ^{44}Ar ($\log_{10} T_{1/2} = 24.065$ s) from ^{252}Fm have the smallest half-life values, which is due to the presence of the near doubly magic clusters with $N \approx 28$, $Z \approx 20$ and it indicates the role of doubly magic ^{208}Pb daughter ($N = 126, Z = 82$). The lowest half-life for ^{48}Ca ($\log_{10} T_{1/2} = 24.045$ s) from ^{254}Fm, ^{50}Ca ($\log_{10} T_{1/2} = 22.181$ s) from ^{256}Fm and ^{52}Ca ($\log_{10} T_{1/2} = 24.255$ s) from ^{258}Fm are obtained, which is due to the presence of doubly or near doubly magic clusters ^{48}Ca ($N = 28, Z = 20$) and stress the role of near double magicity of the ^{206}Hg daughter nuclei ($N = 126, Z \approx 82$).

Figure 3 shows the variation of logarithm of barrier penetrability with mass number for various clusters emitted from $^{244-260}$Fm isotopes. It is found that in the case of ^{46}Ar and ^{48,50}Ca, barrier penetrability has a large value (compared to other clusters) and all these cases refer to doubly magic ^{208}Pb daughter or neighbouring one. In the case of ^{46}Ar emission, penetrability increases as it approaches the doubly closed shell ^{208}Pb daughter. Similar result is obtained for ^{48,50}Ca emission which stresses the role of near doubly magic ^{206}Hg daughter with $N = 126$ and $Z \approx 82$. That is, shell structure effects are evident in these plots in terms of maxima (largest penetrability value) or coming up of all plots compared to other clusters.

Figure 4 represents the computed half-life vs. neutron number of daughter nuclei for $^{244-260}$Fm isotopes emitting clusters ranging from ^{4}He to ^{70}Ni. The computed alpha decay half-lives are in good agreement with the experimental data. Experimental alpha half-life values are taken from Royer [46]. In this plot a dip is obtained at neutron number $N = 126$, which indicates the neutron shell closure of daughter nuclei at $N = 126$.

The nuclear proximity potential for oriented and deformed (with higher multipole deformation) nuclei are done following the prescription of Gupta and coworkers [41]

Table 2. The computed half-life values, barrier penetrability and other characteristics of $^{252-260}$Fm isotopes with zero angular momentum transfers. Here the interacting potential is taken as $V_C + V_p$.

Parent nuclei	Emitted cluster	Daughter nuclei	Q-value (MeV)	Penetrability P	Decay constant	$\log_{10}(T_{1/2})$	
						Present I	Present II
^{252}Fm	^{4}He	^{248}Cf	7.152	1.99E-27	6.55E-07	6.025	5.712
	^{44}Ar	^{208}Pb	131.239	8.41E-47	1.72E-25	24.065	23.166
	^{46}Ar	^{206}Pb	130.322	2.32E-47	8.19E-26	24.927	23.470
	^{48}Ca	^{204}Hg	145.722	1.31E-47	5.15E-26	25.129	23.433
	^{50}Ca	^{202}Hg	143.734	1.01E-49	3.94E-28	27.246	25.653
^{254}Fm	^{4}He	^{250}Cf	7.307	9.46E-27	3.18E-06	5.339	4.992
	^{44}Ar	^{210}Pb	128.306	9.69E-52	3.43E-30	29.306	27.944
	^{46}Ar	^{208}Pb	132.373	2.52E-43	9.04E-22	20.306	19.338
	^{48}Ca	^{206}Hg	146.065	1.58E-46	6.25E-25	24.045	23.739
	^{50}Ca	^{204}Hg	145.165	1.11E-46	4.34E-25	24.203	22.455
	^{52}Ca	^{202}Hg	140.750	2.37E-53	9.03E-32	30.885	29.355
^{256}Fm	^{4}He	^{252}Cf	7.027	6.07E-28	1.96E-07	6.548	6.218
	^{46}Ar	^{210}Pb	129.934	1.29E-47	4.54E-26	25.183	23.361
	^{48}Ar	^{208}Pb	130.955	3.69E-44	1.31E-22	21.724	20.177
	^{50}Ca	^{206}Hg	146.003	1.16E-44	4.57E-23	22.181	26.105
	^{52}Ca	^{204}Hg	142.676	2.22E-49	8.56E-28	26.908	25.286
	^{54}Ti	^{202}Pt	155.476	1.24E-52	5.22E-31	30.123	29.840
^{258}Fm	^{4}He	^{254}Cf	6.664	1.31E-29	4.02E-09	8.237	7.928
	^{46}Ar	^{212}Pb	127.697	6.93E-51	2.40E-27	28.461	27.051
	^{48}Ar	^{210}Pb	128.878	1.48E-47	5.18E-26	25.127	23.640
	^{50}Ca	^{208}Hg	126.679	1.77E-50	6.08E-29	28.057	25.421
	^{52}Ca	^{206}Hg	143.876	9.90E-47	3.86E-25	24.255	22.527
	^{54}Ti	^{204}Pt	154.660	1.22E-53	5.11E-32	31.132	29.338
^{260}Fm	^{4}He	^{256}Cf	6.175	3.43E-32	9.63E-12	10.854	10.474
	^{48}Ar	^{212}Pb	126.907	4.90E-52	1.69E-30	29.614	26.946
	^{50}Ca	^{210}Hg	140.321	4.32E-54	1.64E-32	31.625	29.467
	^{52}Ca	^{208}Hg	141.240	3.74E-51	1.43E-29	28.685	30.121
	^{54}Ca	^{206}Hg	140.476	2.49E-51	9.49E-30	28.864	27.264

with universal proximity potential given in eqs (4) and (5). In fission and cluster decay the fragments are strongly polarized due to nuclear force and accordingly their symmetry axes are aligned. In the present work we consider only pole to pole configuration. We have studied the effect of quadrupole deformation β_2 and hexadecapole deformation β_4 of the parent, daughter and emitted cluster on half-life. The deformations β_2 and β_4 are taken from [48]. Tables 3 and 4 give the comparison of calculated values of the logarithm of half-life without deformation (a), with quadrupole deformation (b) and with deformations β_2 and β_4 (c). It is found that inclusion of β_2 and β_4 reduces the height and shape of the barrier (increases barrier penetrability) and hence the half-life decreases.

Table 3. The comparison of calculated values of the logarithm of half-life without deformation (a), with quadrupole deformation (b) and with deformations β_2 and β_4(c).

			Parent		Deformation cluster		Daughter		$\mathrm{Log}_{10}(T_{1/2})$		
Parent nuclei	Emitted cluster	Q value (MeV)	β_2	β_4	β_2	β_4	β_2	β_4	a	b	c
^{244}Fm	^{4}He	8.555	0.224	0.071	0.000	0.000	0.215	0.085	0.315	−1.402	−2.711
	^{8}Be	16.178	0.224	0.071	0.000	0.000	0.215	0.102	24.773	20.867	17.705
	^{12}C	30.644	0.224	0.071	0.000	0.000	0.208	0.117	27.876	22.099	16.757
	^{32}Si	101.750	0.224	0.071	0.000	0.000	0.000	0.008	24.007	21.190	18.422
	^{34}Si	98.837	0.224	0.071	0.000	0.000	0.000	0.008	28.162	25.321	22.517
	^{36}S	118.540	0.224	0.071	0.000	0.000	−0.018	−0.008	22.441	21.135	19.045
	^{38}S	114.050	0.224	0.071	0.000	0.000	−0.018	−0.008	29.969	27.334	25.050
	^{42}Ar	129.360	0.224	0.071	0.000	0.000	0.008	−0.008	29.441	24.765	23.987
	^{48}Ca	145.050	0.224	0.071	0.000	0.000	−0.122	−0.032	26.756	29.529	26.177
^{246}Fm	^{4}He	8.375	0.234	0.057	0.000	0.000	0.224	0.079	0.913	−0.929	−2.137
	^{8}Be	15.798	0.234	0.057	0.000	0.000	0.215	0.093	26.090	22.118	19.282
	^{12}C	29.790	0.234	0.057	0.000	0.000	0.216	0.109	29.949	23.882	18.969
	^{32}Si	98.540	0.234	0.057	0.000	0.000	0.008	0.008	29.226	25.150	22.668
	^{34}Si	98.757	0.234	0.057	0.000	0.000	0.000	0.008	27.980	24.943	22.573
	^{36}S	116.760	0.234	0.057	0.000	0.000	0.000	0.008	25.947	22.329	19.637
	^{38}S	115.870	0.234	0.057	0.000	0.000	−0.018	−0.008	26.325	24.024	22.511
	^{48}Ca	145.310	0.234	0.057	0.000	0.000	−0.122	−0.032	25.776	28.313	26.054
^{248}Fm	^{4}He	8.001	0.235	0.049	0.000	0.000	0.234	0.073	2.262	0.282	−0.845
	^{8}Be	15.239	0.235	0.049	0.000	0.000	0.224	0.087	28.170	24.014	21.365
	^{38}S	114.720	0.235	0.049	0.000	0.000	0.000	0.008	28.009	24.556	22.172
	^{40}S	113.630	0.235	0.049	0.254	−0.001	−0.018	−0.008	28.902	11.763	12.591
	^{46}Ar	127.560	0.235	0.049	0.000	0.000	0.008	−0.008	29.309	26.584	25.824
	^{48}Ca	145.630	0.235	0.049	0.000	0.000	−0.113	−0.033	24.666	27.167	25.856
	^{50}Ca	142.430	0.235	0.049	0.000	0.000	−0.122	−0.032	29.031	31.598	29.984
^{250}Fm	^{4}He	7.557	0.235	0.033	0.000	0.000	0.234	0.057	3.996	1.968	1.074
	^{8}Be	14.327	0.235	0.033	0.000	0.000	0.224	0.079	31.876	27.645	25.299
	^{40}S	112.880	0.235	0.033	0.254	−0.001	0.000	0.008	29.913	10.313	10.278
	^{42}Cl	120.730	0.235	0.033	0.218	−0.016	−0.018	−0.008	29.696	12.835	14.672
	^{44}Ar	130.540	0.235	0.033	0.000	0.000	−0.008	−0.008	24.819	21.988	21.678
	^{46}Ar	128.900	0.235	0.033	0.000	0.000	−0.008	−0.008	26.436	23.806	23.559
	^{48}Ca	145.640	0.235	0.033	0.000	0.000	−0.087	−0.035	24.119	25.692	26.348
	^{50}Ca	143.150	0.235	0.033	0.000	0.000	−0.113	−0.033	27.221	29.907	29.915

We have computed the branching ratio with respect to alpha decay for all clusters. The branching ratio is given by

$$B = \frac{\lambda_{\mathrm{cluster}}}{\lambda_{\mathrm{alpha}}} = \frac{T_{1/2}^{\mathrm{alpha}}}{T_{1/2}^{\mathrm{cluster}}}. \tag{17}$$

We would like to mention that using the presently available techniques in cluster radioactivity, it is possible to measure half-life values up to 10^{30} s and branching ratio as low as 10^{-19} [49]. For computing branching ratios, experimental alpha half-life values are taken from Royer [46]. Branching ratio calculations also reveal

Table 4. The comparison of calculated values of logarithm of the half-life without deformation (a), with quadrupole deformation (b) and with deformations β_2 and β_4 (c).

			Deformation								
			Parent		cluster		Daughter		$\text{Log}_{10}(T_{1/2})$		
Parent nuclei	Emitted cluster	Q value (MeV)	β_2	β_4	β_2	β_4	β_2	β_4	a	b	c
^{252}Fm	^{4}He	7.152	0.245	0.018	0.000	0.000	0.235	0.040	5.712	3.629	2.990
	^{44}Ar	131.240	0.245	0.018	0.000	0.000	0.000	0.000	23.166	19.893	19.330
	^{46}Ar	130.320	0.245	0.018	0.000	0.000	−0.008	−0.008	23.470	21.074	21.424
	^{48}Ca	145.720	0.245	0.018	0.000	0.000	−0.061	−0.037	23.433	23.554	25.874
	^{50}Ca	143.730	0.245	0.018	0.000	0.000	−0.087	−0.035	25.653	27.180	28.937
^{254}Fm	^{4}He	7.307	0.237	0.008	0.000	0.000	0.245	0.026	4.992	2.833	2.421
	^{44}Ar	128.310	0.237	0.008	0.000	0.000	0.000	0.008	27.944	24.080	22.889
	^{46}Ar	132.370	0.237	0.008	0.000	0.000	0.000	0.000	19.338	17.261	17.062
	^{48}Ca	146.070	0.237	0.008	0.000	0.000	−0.008	0.000	23.739	19.729	19.456
	^{50}Ca	145.170	0.237	0.008	0.000	0.000	−0.061	−0.037	22.455	23.721	27.087
	^{52}Ca	140.750	0.237	0.008	0.000	0.000	−0.087	−0.035	29.355	31.053	33.635
^{256}Fm	^{4}He	7.027	0.227	−0.003	0.000	0.000	0.236	0.015	6.218	4.119	3.885
	^{46}Ar	129.930	0.227	−0.003	0.000	0.000	0.000	0.008	23.361	20.848	20.932
	^{48}Ar	30.960	0.227	−0.003	−0.207	−0.067	0.000	0.000	20.177	30.975	35.059
	^{50}Ca	146.000	0.227	−0.003	0.000	0.000	−0.008	0.000	26.105	18.790	18.779
	^{52}Ca	142.680	0.227	−0.003	0.000	0.000	−0.061	−0.037	25.286	26.778	30.998
	^{54}Ti	155.480	0.227	−0.003	0.000	0.000	−0.061	−0.037	29.840	28.803	33.117
^{258}Fm	^{4}He	6.664	0.228	−0.019	0.000	0.000	0.226	0.005	7.928	5.889	5.825
	^{46}Ar	127.700	0.228	−0.019	0.000	0.000	0.000	0.008	27.051	23.963	23.488
	^{48}Ar	128.880	0.228	−0.019	−0.207	−0.067	0.000	0.008	23.640	33.435	37.534
	^{50}Ca	126.680	0.228	−0.019	0.000	0.000	−0.008	0.000	25.421	48.592	49.708
	^{52}Ca	143.880	0.228	−0.019	0.000	0.000	−0.008	0.000	22.527	20.863	21.412
	^{54}Ti	154.660	0.228	−0.019	0.000	0.000	0.008	0.000	29.338	24.700	25.391
^{260}Fm	^{4}He	6.175	0.219	−0.030	0.000	0.000	0.218	−0.005	10.474	8.472	8.583
	^{8}Be	14.638	0.219	−0.030	0.000	0.000	0.226	0.012	30.230	26.074	25.938
	^{48}Ar	126.910	0.219	−0.030	−0.207	−0.067	0.000	0.008	26.946	36.362	42.691
	^{50}Ca	140.320	0.219	−0.030	0.000	0.000	−0.026	−0.008	29.467	28.201	30.525
	^{52}Ca	141.240	0.219	−0.030	0.000	0.000	−0.008	0.000	30.121	24.859	25.825
	^{54}Ca	140.480	0.219	−0.030	0.000	0.000	−0.008	0.000	27.264	25.364	26.256
	^{56}Ti	153.220	0.219	−0.030	0.135	−0.018	0.008	0.000	31.718	14.275	17.487

that ^{44,46}Ar, ^{48}Ca from ^{252}Fm; ^{46}Ar ,^{50}Ca from ^{254}Fm;^{46,48}Ar from ^{256}Fm;^{48}Ar, ^{50,52}Ca from ^{258}Fm and ^{48}Ar, ^{50,52}Ca from ^{260}Fm are favourable for measurements in on-line experiments, e.g. ^{48}Ar ($B = 8.57 \times 10^{-16}$) from ^{256}Fm and ^{52}Ca ($B = 3.89 \times 10^{-15}$) from ^{258}Fm. Radioactive beams could be used to produce these parent nuclei.

When the decay of ^{44}Ar from ^{252}Fm is compared with that from heavier isotopes up to ^{260}Fm, it is evident that the logarithm of half-life values increases from 24.065 s (for ^{252}Fm, $Q = 131.239$ MeV) to 43.817 s (for ^{260}Fm, $Q = 120.493$ MeV). All these cases refer to the doubly or near doubly magic ^{208}Pb daughter. Also when ^{46}Ar emission from ^{254}Fm is compared with that from heavier isotopes up to ^{260}Fm,

it is evident that the logarithm of half-life values increases from 20.306 s (for ^{254}Fm, $Q = 132.373$ MeV) to 34.123 s (for ^{260}Fm, $Q = 125.179$ MeV). A similar result is obtained for ^{48}Ar emission also. The logarithm of half-lives increases from 21.724 s (for ^{256}Fm, $Q = 130.995$ MeV) to 29.614 s (for ^{260}Fm, $Q = 126.907$ MeV). These cases also refer to the doubly or near doubly magic ^{208}Pb daughter. From these we would like to point out that neutron excess in the parent nuclei slows down the cluster decay process.

Acknowledgement

One of the authors (KPS) would like to thank the University Grants Commission, Govt. of India for the financial support under Project No. MRP(S)-352/2005(X Plan)/KLKA 002/UGC-SWRO.

References

[1] A Sandulescu, D Poenaru and W Greiner, *Sov. J. Part. Nucl.* **II**, 528 (1980)
[2] R K Gupta, in *Heavy elements and related new phenomena* edited by W Greiner and R K Gupta (World Scientific Pub., Singapore, 1999) Vol. I, p. 536
[3] H J Rose and G A Jones, *Nature (London)* **307**, 245 (1984)
[4] R Bonetti and A Guglielmetti, in: *Heavy elements and related new phenomena* edited by W Greiner and R K Gupta (World Scientific Pub., Singapore, 1999) Vol. II, p. 643
[5] D N Poenaru, M Ivascu, A Sandulescu and W Greiner, *J. Phys. G: Nucl Part. Phys.* **10**, L183 (1984)
[6] D N Poenaru, M Ivascu, A Sandulescu and W Greiner, *Phys. Rev.* **C32**, 572 (1985)
[7] D N Poenaru, W Greiner, A Sandulescu and M Ivascu, *Phys. Rev.* **C32**, 2198 (1985)
[8] W Greiner, M Ivascu, D N Poenaru and A Sandulescu, *Z. Phys.* **A320**, 347 (1985)
[9] Y J Shi and W J Swiatecki, *Phys. Rev. Lett.* **54**, 300 (1985)
[10] A Sandulescu, D N Poenaru, W Greiner and J H Hamilton, *Phys. Rev. Lett.* **54**, 490 (1985)
[11] G A Pik-Pichak, *Sov. J. Nucl. Phys.* **44**, 923 (1986)
[12] G Shanmugam and B Kamalaharan, *Phys. Rev.* **C38**, 1377 (1988)
[13] B Buck and A C Merchant, *J. Phys. G: Nucl. Part. Phys.* **15**, 615 (1989)
[14] K P Santhosh and Antony Joseph, *Ind. J. Pure & Appl. Phys.* **42**, 806 (2004)
[15] K P Santhosh and Antony Joseph, *Pramana – J. Phys.* **55**, 375 (2000)
[16] G Royer, R K Gupta and V Yu Denisov, *Nucl. Phys.* **A632**, 275 (1998)
[17] S Landowne and C H Dasso, *Phys. Rev.* **C33**, 387 (1986)
[18] M Iriondo, D Jerrestan and R J Liotta, *Nucl. Phys.* **A454**, 252 (1986)
[19] R Blendoaske, T Fliessbach and H Walliser, *Nucl. Phys.* **A464**, 75 (1987)
[20] S S Malik and R K Gupta, *Phys. Rev.* **C39**, 1992 (1989)
[21] S Kumar and R K Gupta, *Phys. Rev.* **C55**, 218 (1997)
[22] M Jones, R P Schuman, J P Butler, G Cowper, T A Eastwood and H G Jackson, *Phys. Rev.* **102**, 203 (1956)
[23] E K Hulet, R W Hoff, J E Evans and R W Lougheed, *Phys. Rev. Lett.* **13**, 343 (1964)
[24] T Sikkeland, A Ghiorso, R Latimer and A E Larsh, *Phys. Rev.* **140**, B277 (1965)
[25] K P Santhosh and Antony Joseph, *Proc. Int. Natl. Symp. Nucl. Phys. (India)* **B43**, 296 (2000)

[26] K P Santhosh and Antony Joseph, *Pramana – J. Phys.* **58**, 611 (2002)
[27] K P Santhosh and Antony Joseph, *Pramana – J. Phys.* **62**, 957 (2004)
[28] K P Santhosh, R K Biju, Sabina Sahadevan and Antony Joseph, *Phys. Scr.* **77**, 065201 (2008)
[29] A Guglielmetti *et al*, *Nucl. Phys.* **A583**, 867c (1995)
[30] A Guglielmetti *et al*, *Phys. Rev.* **C56**, R2912 (1997)
[31] M La Commara *et al*, *Nucl. Phys.* **A669**, 43 (2000)
[32] K P Santhosh and Antony Joseph, *Pramana – J. Phys.* **59**, 679 (2002)
[33] R K Biju, Sabina Sahadevan, K P Santhosh and Antony Joseph, *Pramana – J. Phys.* **70**, 617 (2008)
[34] K P Santhosh, R K Biju and Antony Joseph, *J. Phys. G: Nucl. Part. Phys.* **35**, 085102 (2008)
[35] Bir Bikram Singh, Sham K Arun, Manoj K Sharma, Shefali Kanwar and Raj K Gupta, *Proc. DAE Symp. Nucl. Phys. (India)* **53**, 261 (2008)
[36] Sham K Arun and Raj K Gupta, *Proc. DAE Symp. Nucl. Phys. (India)* **52**, 365 (2007)
[37] M K Sharma, B B Singh and R K Gupta, *Proc. 11th Punjab Science Congress* (2008) p. 40
[38] J Blocki, J Randrup, W J Swiatecki and C F Tsang, *Ann. Phys. (N.Y.)* **105**, 427 (1977)
[39] J Blocki and W J Swiatecki, *Ann. Phys. (N.Y.)* **132**, 53 (1981)
[40] C Y Wong, *Phys. Rev. Lett.* **31**, 766 (1973)
[41] N Malhotra and R K Gupta, *Phys. Rev.* **C31**, 1179 (1985)
[42] R K Gupta, M Balasubramaniam, R Kumar, N Singh, M Manhas and W Greiner, *J. Phys. G: Nucl. Part. Phys.* **31**, 631 (2005)
[43] Y J Shi and W J Swiatecki, *Nucl. Phys.* **A438**, 450 (1985)
[44] G Audi, A H Wapstra and C Thivault, *Nucl. Phys.* **A729**, 337 (2003)
[45] H Koura, T Tachibana, M Uno and M Yamada, *Prog. Theor. Phys.* **113**, 305 (2005)
[46] G Royer, *J. Phys. G: Nucl. Part. Phys.* **26**, 1149 (2000)
[47] R K Gupta and W Greiner, *Int. J. Mod. Phys.* **E3**, 335 (1994)
[48] P Moller, J R Nix, W D Myers and W J Swiatecki, *At. Data Nucl. Data Tables* **59**, 185 (1995)
[49] S Wang, D Snowden-Ifft, P B Price, K J Moody and E K Hulet, *Phys. Rev.* **C39**, 1647 (1989)